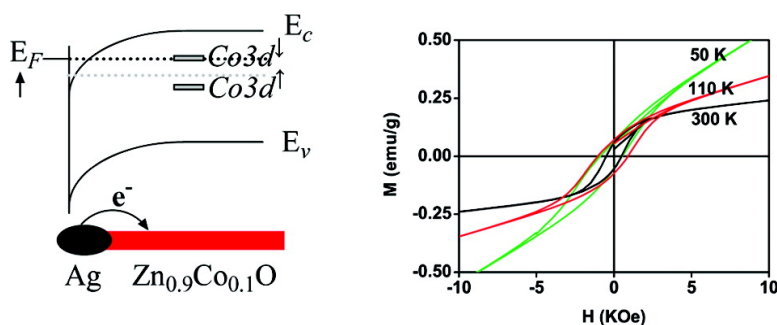


Metal–Semiconductor Hybrid Nanostructure Ag–ZnCoO: Synthesis and Room-Temperature Ferromagnetism

Xiaoqing Qiu, Liping Li, Changlin Tang, and Guangshe Li

J. Am. Chem. Soc., **2007**, 129 (39), 11908–11909 • DOI: 10.1021/ja074630d • Publication Date (Web): 11 September 2007

Downloaded from <http://pubs.acs.org> on February 14, 2009



More About This Article

Additional resources and features associated with this article are available within the HTML version:

- Supporting Information
- Links to the 4 articles that cite this article, as of the time of this article download
- Access to high resolution figures
- Links to articles and content related to this article
- Copyright permission to reproduce figures and/or text from this article

[View the Full Text HTML](#)

Metal–Semiconductor Hybrid Nanostructure Ag–Zn_{0.9}Co_{0.1}O: Synthesis and Room-Temperature Ferromagnetism

Xiaoqing Qiu, Liping Li, Changlin Tang, and Guangshe Li*

State Key Lab of Structural Chemistry, Fujian Institute of Research on the Structure of Matter and Graduate School of Chinese Academy of Sciences, Fuzhou 350002, People's Republic of China

Received June 25, 2007; E-mail: guangshe@fjirsm.ac.cn

Preparation of ZnO-based semiconductors of various crystalline forms has been extensively studied with a goal of achieving room-temperature ferromagnetism (FM) for applications in spintronics.¹ However, the reproducibility of FM is very poor, and the nature of FM is not clear.^{1c} Free carriers have been reported in the literature as one of the causes for ferromagnetic order,² which are always metastable and strongly disturbed by experimental conditions. As a consequence, it is very difficult to obtain stable and reproducible room-temperature FM using the conventional methodologies.³

Metal–semiconductor hybrid nanostructure provides a unique opportunity to stably achieve room-temperature FM since metallic decoration may tune the Fermi level⁴ of semiconductors and promote the electron transfer to induce ferromagnetic ordering.⁵ Nevertheless, it is still a challenge to prepare metal–semiconductor hybrid nanostructure for room-temperature FM.⁶ In this communication, we initiated the preparation of hybrid nanostructure Ag–Zn_{0.9}Co_{0.1}O based on the following considerations: (1) Zn_{0.9}Co_{0.1}O nanorods have a polar surface structure, and thus it is highly possible to attach small Ag nanocrystals on the “activated centers” of the top or the wall of the nanorods. The surface energy of the negatively charged plane of O²⁻ ions for nanorods is higher than that of the nonpolar planes⁷ and, therefore, is energetically favored by attaching exotic species to form a heterostructure;⁸ the stacking faults of Zn_{0.9}Co_{0.1}O parallel to the [0001] direction could act as the activated centers for promoting massive surface reconstructions.⁹ (2) Most importantly, Co²⁺ doping in ZnO nanorods can produce a significant red shift in band gap energy¹⁰ in favor of the electron transfer from Ag nanocrystals to tune the Fermi level of ZnO. We prepared Ag–Zn_{0.9}Co_{0.1}O hybrid nanostructure via a solution chemistry and discovered an abnormally large room-temperature FM which shows a promising application as a novel diluted magnetic semiconductor. Details of the sample preparations and characterizations are given in Supporting Information.

X-ray diffraction (Figure S1) indicated that the majority phase of as-prepared samples is a hexagonal lattice. When Ag species were involved in the reaction systems, no Co clusters were observed but a secondary phase of silver was observed. All lattice parameters of the majority phase were slightly smaller than those of pure ZnO, indicating the formation of a solid solution Zn_{0.9}Co_{0.1}O (Figure S1). Since XRD technique has a detection limit of 5% and minor magnetic impurities can yield a huge impact on the total magnetic properties, we did a parallel experiment under the identical conditions with no Zn²⁺. We found that the products consisted of β-Co(OH)₂ and Ag in the presence of a minor phase of Co₃O₄. Since ethanol solvent at 120 °C has a very low reduction activity, Co ions are difficult to reduce to metallic clusters.¹¹ Our X-ray photoelectron spectroscopy confirmed the absence of metallic Co in our samples (Figure S2). Therefore, Co clusters as previously

reported in the literature^{1d,e} can be dismissed from the effects to the robust FM in Ag–Zn_{0.9}Co_{0.1}O hybrid nanostructure as described later.

TEM images indicated that all samples were composed of nanorods with their wall or top being attached by nanocrystals (Figure 1 and Figure S3). EDX analysis (Figure S4) confirmed that these nanocrystals and nanorods were silver and Zn_{0.9}Co_{0.1}O, respectively. These results indicated the formation of a metal–semiconductor hybrid nanostructure. Many more TEM images of individual hybrid nanostructure are clearly seen in Figure S3. A high-resolution TEM image of individual hybrid nanostructure showed that the regular spacing of lattice planes for the Ag nanoparticle is 0.236 nm, which is compatible with that of Ag-(111) planes, while the interplanar spacing of Zn_{0.9}Co_{0.1}O nanorods was 0.285 nm, much closer to that between two adjacent (100) planes of ZnO. Further, EDX line scanning analysis along nanorods indicated a homogeneous distribution of Co and Zn (Figure S4).

Electronic structure of Ag–Zn_{0.9}Co_{0.1}O hybrid nanostructure was examined by diffusion reflection spectroscopy. As illustrated in Figure 2a, besides the intrinsic exciton band at 368 nm for pure ZnO nanorods, Ag(4%)–Zn_{0.9}Co_{0.1}O hybrid nanostructure showed two additional absorption bands in the ranges of 500–400 and 700–500 nm in comparison with pure ZnO nanorods. The first band is ascribed to the silver plasma band.⁸ To uncover the nature of the second one, the absorptions observed in the wavelength range from 720 to 500 nm for hybrid nanostructure are enlarged (Figure 2b). The absorptions for pure ZnO and Zn_{0.9}Co_{0.1}O nanorods were also given for comparison. Three absorption peaks were observed at about 660, 566, and 609 nm for both Ag–Zn_{0.9}Co_{0.1}O hybrid nanostructure and Zn_{0.9}Co_{0.1}O nanorods, which are characteristic of the transitions of ⁴A₂(F)–²E(G), ⁴A₂(F)–⁴T₁(P), and ⁴A₂(F)–²A₁(G), respectively, for high-spin Co²⁺ (3d⁷) in a tetrahedral coordination.^{1a,d} Strikingly, the presence of Ag nanocrystals in the hybrid nanostructure reduced the Co²⁺ ligand-field absorbance to show an apparent bleaching effect (Figure 2b), just like what is reported in Co²⁺:ZnO film after treatment in Zn vapor.^{2b} Therefore, part of the electrons that transfer from Ag nanocrystals might be introduced and accumulated in Zn_{0.9}Co_{0.1}O nanorods^{4b,c} to interact strongly with Co²⁺ ions. The subsequent electron delocalization among Co²⁺ ions may favor to the generation of FM.

Ag–Zn_{0.9}Co_{0.1}O hybrid nanostructure showed room-temperature FM, as indicated by the well-defined hysteresis loops (Figure 3a). The coercivities are 0.49 KOe for 1% Ag and 0.31 KOe for 4% Ag, which are all several times larger than those reported for Zn_{1-x}Co_xO nanostructures of films,^{1b} nanoparticles,^{2c} and nanorods.^{1f} No saturation magnetization was reached even under an external magnetic field of 8 T, which indicates the presence of a ferromagnetic component superimposed with a paramagnetic one. Paramagnetic and ferromagnetic components were distinguished using the modified Langevin function for initial magnetization curves (Figure

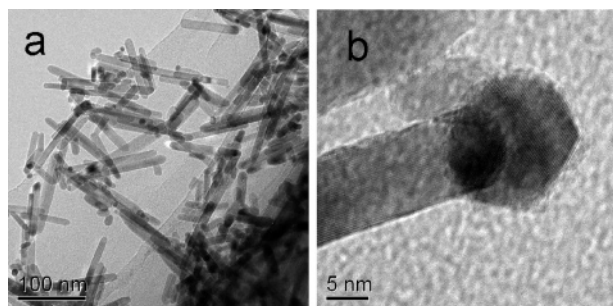


Figure 1. (a) TEM image of 4% Ag–Zn_{0.9}Co_{0.1}O hybrid nanostructure and (b) high-resolution TEM image of individual hybrid nanostructure.

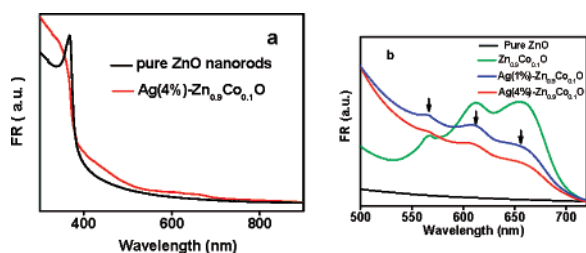


Figure 2. (a) Diffusion reflection spectra of Ag(4%)–Zn_{0.9}Co_{0.1}O hybrid nanostructure compared with pure ZnO nanorods and (b) the enlarged ligand-field absorption of Co²⁺ for given samples.

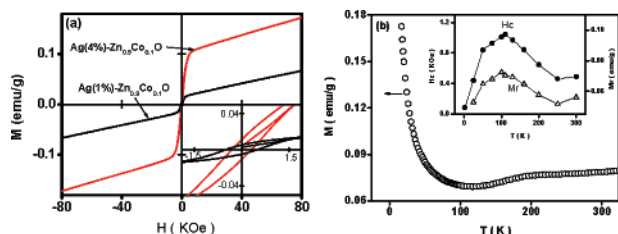


Figure 3. (a) Room-temperature M – H curves of Ag–Zn_{0.9}Co_{0.1}O hybrid nanostructure at different Ag content and (b) temperature dependence of magnetization of Ag(1%)–Zn_{0.9}Co_{0.1}O under $H = 1000$ Oe. Inset (a) shows the enlarged magnetization curves, and inset (b) is temperature dependence of coercivity and remanence.

S5). It is found that the magnetic susceptibility of the paramagnetic component followed a Curie–Weiss relationship showing a Curie–Weiss constant of 0.0021 emu/g, which is much closer to that for pure Zn_{0.9}Co_{0.1}O nanorods (Figure S6). Therefore, the paramagnetic component is intrinsic for Zn_{0.9}Co_{0.1}O nanorods. We also did a comparative study on the temperature dependence of magnetization for Zn_{0.9}Co_{0.1}O nanorods with and without a Ag tip. As indicated in Figure 3b, with decreasing temperature, the magnetization of Ag–Zn_{0.9}Co_{0.1}O hybrid nanostructure decreased to show a minimum at about 110 K, which is different from the paramagnetic Zn_{0.9}Co_{0.1}O nanorods (Figure S6). Inset of Figure 3b gives the temperature dependence of coercivity and remanence for Ag(1%)–Zn_{0.9}Co_{0.1}O hybrid nanostructure. It is seen that the coercivity increased up to 110 K and decreased slowly as temperature increased and then was kept as a constant. This finding is probably associated with the increased free carrier concentrations.

According to the Zener model, ferromagnetic interaction between the localized Co²⁺ moments is mediated by the delocalized carriers. The bleaching effect of the Co²⁺ ligand-field absorption and exciton band (Figure 2b) indicated the electron transfer from Ag to Co²⁺. It is well-known that the band gap for bulk ZnO is 3.2 eV in which the up-spin d states of Co²⁺ are fully occupied, while down-spin

ones are partially filled. The Fermi level lies in a gap between the crystal field split (Figure S7). Because the direction of electron transfer between metal and semiconductor is determined by the relative work function, here we compared the work functions of Ag nanocrystals and Zn_{0.9}Co_{0.1}O nanorods. The work function is a sum of electron affinity, E_a , and one-half of band gap, E_g . As a first approximation, the electron affinity of Zn_{0.9}Co_{0.1}O nanorods is assumed to be 4.5 eV as for bulk ZnO.¹² Therefore, the work function of Zn_{0.9}Co_{0.1}O nanorods is larger than that of 4.2 eV for metal Ag.¹² On the basis of the difference in work function, we proposed that Ag nanoparticles donated electrons which transfer to and accumulate in semiconductor Zn_{0.9}Co_{0.1}O nanorods, most likely shifting the Fermi level to the down-spin states and slightly overlapping with the conduction band at the edge (Figure S7). This explanation is indirectly verified by Coey et al. who concluded that ZnO-based diluted semiconductors exhibit ferromagnetic behavior when 3d states of the transition element hybridize with the spin-split impurity-band states of carriers at the Fermi level.¹³ The magnetic interactions between the localized spins in the hybrid nanostructure were probably enhanced by such an electron transfer. Similar mechanism has also been proposed for carbon nanospheres encapsulating silver nanocrystals.¹⁴

Acknowledgment. This work was financially supported by NSFC under Contract No. 20671092, NBRPC (973 program, No. 2007CB613306), Directional program (KJCX2-YW-M05), FFKLN (2006L2005), and a grant from Hundreds Youth Talents Program of CAS (G.L.). G.L. thanks the reviewers for critical reading of the manuscript and for their important comments.

Supporting Information Available: XRD, XPS, EDX, TEM, M – H , and χ_g – T curves, and schematic level diagram of Zn_{0.9}Co_{0.1}O nanorods with and without a Ag tip. This material is available free of charge via the Internet at <http://pubs.acs.org>.

References

- (1) (a) Kim, K. J.; Park, Y. R. *Appl. Phys. Lett.* **2002**, *81*, 1420. (b) Lee, H. J.; Jeong, S. Y.; Cho, C. R.; Park, C. H. *Appl. Phys. Lett.* **2002**, *81*, 4020. (c) Ueda, K.; Tabata, H.; Kawai, T. *Appl. Phys. Lett.* **2001**, *79*, 988. (d) Deka, S.; Joy, P. A. *Appl. Phys. Lett.* **2006**, *89*, 032508. (e) Park, J. H.; Kim, M. G.; Jang, H. M.; Ryu, S.; Kim, Y. M. *Appl. Phys. Lett.* **2004**, *84*, 1338. (f) Yang, L. W.; Wu, X. L.; Qiu, T.; Siu, G. G.; Chu, P. K. *J. Appl. Phys.* **2006**, *99*, 074303.
- (2) (a) Alaria, J.; Bieber, H.; Colis, S.; Schmerber, G.; Dinia, A. *Appl. Phys. Lett.* **2006**, *88*, 112503. (b) Schwartz, D. A.; Gamelin, D. R. *Adv. Mater.* **2004**, *16*, 2115. (c) Jayakumar, O. D.; Gopalakrishnan, I. K.; Kulshreshtha, S. K. *Adv. Mater.* **2006**, *18*, 1857.
- (3) Seshadri, R. *Curr. Opin. Solid State Mater. Sci.* **2005**, *9*, 1.
- (4) (a) Subramanian, V.; Wolf, E. E.; Kamat, P. V. *J. Am. Chem. Soc.* **2004**, *126*, 4943. (b) Subramanian, V.; Wolf, E. E.; Kamat, P. V. *J. Phys. Chem. B* **2003**, *107*, 7479. (c) Wood, A.; Giersig, M.; Mulvaney, P. *J. Phys. Chem. B* **2001**, *105*, 8810.
- (5) (a) Spaldin, N. A. *Phys. Rev. B* **2004**, *69*, 125201. (b) Hu, S. J.; Yan, S. S.; Zhao, M. W.; Mei, L. M. *Phys. Rev. B* **2006**, *73*, 245205.
- (6) (a) Casavola, M.; Grillo, V.; Carlino, E.; Giannini, C.; Gozzo, F.; Pinel, E. F.; Garcia, M. A.; Manna, L.; Cingolani, R.; Cozzoli, P. D. *Nano Lett.* **2007**, *7*, 1386. (b) Jung, S. W.; Park, W. I.; Yi, G. C.; Kim, M. *Adv. Mater.* **2003**, *15*, 1358. (c) Mokari, T.; Sztrum, C. G.; Salant, A.; Rabani, E.; Banin, U. *Nat. Mater.* **2005**, *4*, 855.
- (7) Diebold, U.; Kopplitz, L. V.; Dulub, O. *Appl. Surf. Sci.* **2004**, *237*, 336.
- (8) Pacholski, C.; Kornowski, A.; Weller, H. *Angew. Chem., Int. Ed.* **2004**, *43*, 4774.
- (9) Li, L. P.; Qiu, X. Q.; Li, G. S. *Appl. Phys. Lett.* **2005**, *87*, 124101.
- (10) Qiu, X. Q.; Li, L. P.; Li, G. S. *Appl. Phys. Lett.* **2006**, *88*, 114103.
- (11) Hirai, H.; Nakao, Y.; Toshima, N. *J. Macromol. Sci., Part A: Pure Appl. Chem.* **1979**, *13*, 727.
- (12) Wang, Z. L.; Song, J. H. *Science* **2006**, *312*, 242.
- (13) Venkatesan, M.; Fitzgerald, C. B.; Lunney, J. G.; Coey, J. M. D. *Phys. Rev. Lett.* **2004**, *93*, 177206.
- (14) Caudillo, R.; Gao, X.; Escudero, R.; Jose-Yacamán, M.; Goodenough, J. B. *Phys. Rev. B* **2006**, *74*, 214418.

JA074630D